PCCP

Accepted Manuscript

ROYAL SOCIETY OF CHEMISTRY

www.rsc.org/pccp

On the Short Circuit Resilience of Organic Solar Cells: Prediction and Validation

A. Jolt Oostra[a]*, Edsger C.P. Smits[b], Dago M. de Leeuw[c,d], Paul W. M. Blom[c], Jasper J. Michels[b,c]

[a)] Zernike Institute for Advanced Materials, University of Groningen, Nijenborgh 4, 9747 AG, Groningen, the Netherlands, e-mail: a.j.oostra@rug.nl

[b)] Holst Centre/TNO, High Tech Campus 31, 5605 KN Eindhoven, the Netherlands

[c)] Max Planck Institute für Polymerforschung, Ackermannweg 10, 55128 Mainz, Germany

Abstract

The operational characteristics of organic solar cells manufactured with large area processing methods suffers from the occurrence of short-circuits due to defects in the photoactive thin film stack. In this work we study the effect of a shunt resistance on an organic solar cell and demonstrate that device performance is not affected negatively as long as the shunt resistance is higher than approximately 1000 Ohm. By studying charge transport across PEDOT:PSS-lithium fluoride/aluminum (LiF/Al) shunting junctions we show that this prerequisite is already met by applying a sufficiently thick (> 1.5 nm) LiF layer. We demonstrate that this remarkable shunt-resilience stems from the formation of a significant charge transport barrier at the PEDOT:PSS-LiF/Al interface. We validate our predictions by fabricating devices with deliberately severed photoactive layers and find an excellent agreement between the calculated and experimental current-voltage characteristics.

1. Introduction

Solution processing of polymeric semiconductors enables low cost "Roll-to-Roll"[1] manufacture of large-area organic light-emitting diodes (OLEDs)[2] and solar cells (OSCs)[3] for flexible lighting, display and energy harvesting applications. Unfortunately, the production yield of such thin-film devices is still suppressed by the occurrence of short circuits associated with processing imperfections and handling damage. This defect-sensitivity stems from the fact that these devices comprise stacks of very thin organic films (*i.e.* typically <100 nm) that are printed or coated on top of each other. The layer stack of an OSC in conventional geometry consists of a (flexible) substrate, an indium tin oxide (ITO) anode, a polymeric hole injection layer of poly(3,4-ethylenedioxythiophene):poly(styrenesulfonate) (PEDOT:PSS), a photoactive blend layer (*e.g.* poly(3-hexylthiophene-2,5-diyl):phenyl-C61-butyric acid methyl ester (P3HT:PCBM)), and a lithium fluoride/aluminum (LiF/Al) cathode. Of these components the PEDOT:PSS and the photoactive layer are processed from solution, whereas the ITO and the cathode are typically applied by low temperature sputtering and thermal evaporation.

In recent work we have shown that the occurrence of short circuits due to defects in the photoactive layer of OLEDs and OSCs, for instance due to film rupture,[4] incomplete wetting,[5] or protrusion of PEDOT:PSS agglomerates,[6] can be prevented by treating the layer stack with aqueous sodium hypochlorite ($NaClO_{(aq)}$) prior to application of the cathode.[6,7] As a result of this treatment the PEDOT:PSS becomes locally over-oxidized and loses its conducting properties in regions where it is exposed.[8] Despite the proven effectiveness of this repair method certain aspects of it may in some cases be considered non-optimal: besides the trivial fact that any repair procedure increases the number of processing steps, we have demonstrated that in case of thiophene-containing photoactive materials, such as P3HT, *local* hypochlorite treatment is

preferred over full-submersion of the stack, as such materials are susceptible to reaction with ClO^- in much the same way as PEDOT.[7] Hence, integration of this repair method in an automated production environment would require a dedicated detection system capable of localizing defects in order to subsequently dispense oxidizing solution in a spatially controlled fashion. It is hence not only out of academic interest to i) quantitatively estimate what the actual effect of a puncture or defect in the photoactive layer would have on device performance, and ii) to investigate possibilities to engineer the cathode in such a way so as to maximize the shunt resistance of the resulting parallel current path without significantly compromising device operation in non-defected regions.

Hence, we commence this work by performing a "paper exercise" modeling an OSC having a perforated photoactive layer with an equivalent circuit comprising a diode, a series resistance, and a parallel resistance element, the latter representing the short circuit caused by the defect. Using experimentally determined input parameters this simple model estimates to what extent device performance is affected by the shunt resistance, which, in turn, is determined by the (lateral) size of the defect and the intrinsic charge transport properties of the cathode-PEDOT:PSS shunting junction. We study the latter in detail by subjecting ITO-PEDOT:PSS-LiF/Al stacks to temperature-resolved current density-voltage (*J-V*) sweeps, while systematically varying nominal LiF thickness. We then compare the measured resistance of PEDOT:PSS-LiF/Al junctions with the model calculations and show that sizable shunt resistances are already obtained for LiF thickness values of the order of 1.5 nm. Finally, we validate our predictions by direct comparison of the calculated *J-V* curves with those measured for OSCs having purposely severed photoactive layers and LiF/Al cathodes with varying LiF thickness.

2. Materials and methods

PEDOT:PSS (Clevios^{tm} P VP AI4083) was purchased from Heraeus and used as received. Glass substrates (30×30 mm^2) pre-patterned with four ITO pixels were cleaned with detergent solution, rinsed with demi-water and treated with an UV-ozone plasma. ITO-PEDOT:PSS-LiF/Al samples were prepared as follows: PEDOT:PSS was spin-coated directly following the UV-ozone treatment and subsequently dried in a vacuum oven at 200 °C for 10 minutes to give dry layers of 100 nm. The substrates were then transferred to a vacuum chamber ($P<5\times10^{-7}$ mBar) where nominally 0 to 2.5 nm lithium fluoride and 100 nm aluminum were applied in a sequential evaporation procedure. The active area of the finished devices was 10.35 mm^2. The samples were characterized in a nitrogen environment using a computer controlled Keithley 2400 SourceMeter. P3HT:PCBM bulk heterojunction solar cells were prepared as described elsewhere.[7] A few of the solar cell pixels were intentionally defected by removing part of the P3HT:PCBM layer with a toluene-soaked swab stick, in order to locally uncover the PEDOT:PSS layer underneath.[7]

3. Results

As mentioned in the introduction, in order to quantify the effect of a short circuit on solar cell performance we model an OSC containing a defect in the photoactive layer with an equivalent parallel circuit comprising i) a diode (*i.e.* representing the non-shunted photoactive device region), ii) an (effective) series resistance element, and iii) a parallel shunt resistance element. If the total device area is considerably larger than the (effective) lateral cross section of the

shunting resistance, the following expression for the measured current density J can be given:[9,10,11]

$$J = J_0\left\{\exp\left[\frac{q(V - JR_sA)}{nkT}\right] - 1\right\} - J_{ph} + \frac{V - JR_sA}{R_{sh}A} \quad (1)$$

The first term on the RHS of Equation (1) represents the diode current, corrected for the photocurrent (J_{ph}) under illuminating conditions, and the second term describes the current through the shunt resistance element (R_{sh}), both corrected for the presence of an effective series resistance (R_s). A represents the total device active surface area and J_0 the dark-saturation current. V is the voltage, q the elementary charge, kT the thermal energy, and n an ideality factor (n = 1 in case of ideal diode characteristics). For the present study it is convenient to express the total parallel shunt resistance R_{sh} as a function of two reciprocally summed contributions:

$$\frac{1}{R_{sh}} = \frac{1}{R_{sh}^{(0)}} + \frac{1}{R_{sh}^{(1)}} \quad (2)$$

Here, $R_{sh}^{(0)}$ represents the "native" shunt resistance of a "pristine" (non-shorted) device, *e.g.* associated with charge carrier recombination as well as microscopic current pathways,[6] perhaps as a consequence of roughness-related issues. $R_{sh}^{(1)}$ relates purely to the presence of an actual macroscopic (hard) short circuit,[7] for instance resulting from handling damage or flawed manufacturing.

In Figure 1 we plot the *JV*-characteristics of two conventional pristine OSCs (ITO-PEDOT:PSS-P3HT:PCBM-LiF/Al), one comprising 2 nm LiF and the other 0.5 nm LiF. The symbols represent measured values (obtained under illumination with AM1.5 simulated solar light[7]) and the lines represent the best fit to Equation (1). The good agreement between model and experiment for $V > -1$ V demonstrates the suitability of the proposed equivalent circuit to describe device behavior in response to a bias within practical bounds. The mechanism behind the enhanced current leakage at high negative bias is neither taken into account by the model, nor of prime interest in the present study.

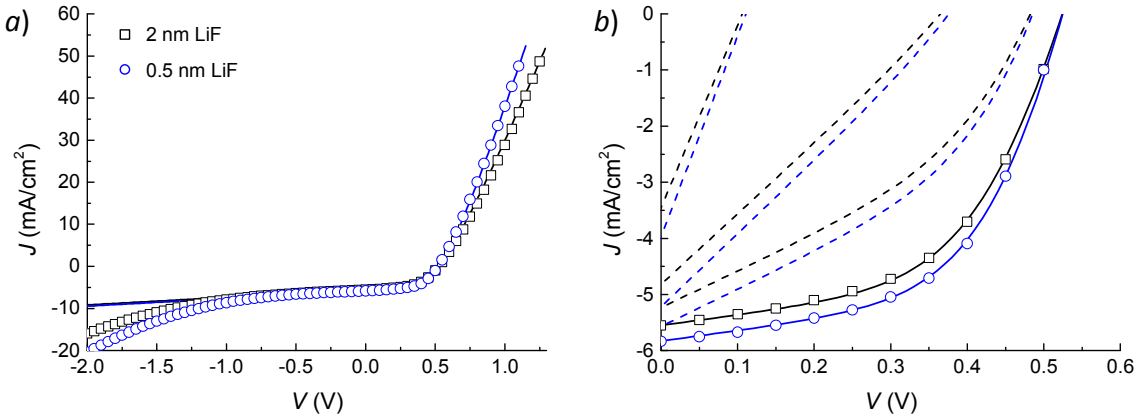

Figure 1. *a) Current density (J) as function of voltage (V) measured (symbols) for OSCs having LiF/Al cathodes with 2 nm and 0.5 nm LiF nominal thickness; solid lines represent a best fit to Equation (1); b) fourth quadrant zoom of the curves; dashed lines represent the calculated JV-characteristics should these same devices contain a shorted region for which* $R_{sh}^{(1)}$ *= 5, 20, and 50* Ω *(left to right).*

The parameter values resulting from the fitting procedure are summarized in Table 1. Besides the values of the effective resistance elements, Table 1 also contains the open circuit voltage (V_{oc}), short circuit current density (J_{sc})[12], fill factor (FF), and light-to-power conversion efficiency (η) of the OSCs. Both cells have similar performance with reasonable efficiencies considering the fairly large active surface area (3.876 cm^2).[7,13] The latter is probably also responsible for the relatively low series resistance R_s. The difference in slope of the first quadrant section of the JV-curves directly shows R_s to increase with LiF thickness. Both curves are fitted with the same ideality factor and native shunt resistance $R_{sh}^{(0)}$, motivated by similar processing and annealing conditions.

Table 1. *Device parameters obtained from curve fitting the JV-data depicted in Figure 1*

d_{LiF} (nm)	V_{oc} (V)	J_{sc} (mA/cm^2)	FF	η (%)	R_s (Ω)	$R_{sh}^{(0)}$ (Ω)	$R_{sh}^{(1)}$ (Ω)	n
2	0.52	-5.55	0.53	1.53	3.1	140	∞	2.3
0.5	0.52	-5.83	0.54	1.65	2.4	140	∞	2.3

For demonstrative purposes Figure 1 includes JV-curves (dashed lines) calculated in case these same OSC devices would suffer from a hard short circuit or puncture giving rise to an additional shunt resistance of $R_{sh}^{(1)}$ = 5, 20, or 50 Ω (from left to right). Obviously, a significant short circuit limits device performance, as expressed by the reduced short open circuit voltage, short circuit current density, and fill factor.[14] The calculations show that the effect of the additional shunt resistance is non-linear: whereas a minimum value of FF ~25% is still observed for for $R_{sh}^{(1)}$ = 20

Ω, device performance seems much less affected for $R_{sh}^{(1)}$ = 50 Ω. In Figure 2 we clarify the effect of the macroscopic short circuit more quantitatively by plotting the calculated fill factor normalized by the value of the pristine device (here: d_{LiF} = 2 nm) as a function of $R_{sh}^{(1)}$. The graph (red curve) demonstrates that in the presence of a macroscopic short circuit over 95% of the native OSC performance is retained as long as $R_{sh}^{(1)}$ is around 1000 Ω.

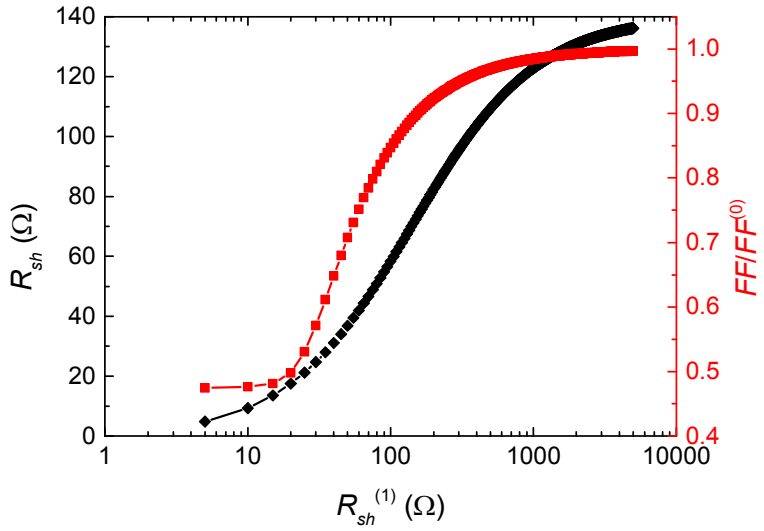

Figure 2. *Calculated (Equation (2)) total shunt resistance (black) and relative fill factor (red) for a 2 nm LiF/Al-based OSC, both plotted as a function of short resistance* $R_{sh}^{(1)}$.

To answer the question whether/under what conditions the shunt resistance resulting from a defect in the photoactive layer would indeed be high enough to avoid the necessity of a separate repair procedure, we measure the resistance of the actual PEDOT:PSS-cathode junctions encountered in defected device regions. Figure 3a plots the current density as a function of voltage recorded for ITO-PEDOT:PSS-LiF/Al stacks (with a surface area of 10.35 mm^2) of

which the nominal thickness of the LiF film is varied in the range 0 – 2.5 nm. The size of these junctions compares well with macroscopic photoactive layer defects expected to result from handling damage or dewetting, and deliberately implemented in OSC devices during our previous investigations.[7] In order to make a comparison with the predictive calculations given above, we plot the resistance measured across the PEDOT:PSS-LiF/Al junctions (denoted R_j) as a function of voltage in Figure 3b.

Strikingly, R_j is strongly dependent on the nominal thickness of the LiF layer, increasing about three orders of magnitude in the experimental range of 0.5 – 2.5 nm. This observation suggests the formation of a significant charge transport barrier, possibly resulting from the formation of dielectric species due to chemical reaction between cathode constituents and PSS and/or residual water present in the PEDOT:PSS layer.[15] The fact that the curves for 0 and 0.5 nm LiF coincide confirms the notion that below a given nominal thickness the LiF film is by no means an integral layer.[16] Assuming that for a device with a perforated or damaged photoactive layer $R_j \approx R_{sh}^{(1)}$, comparison of Figure 3b with the curve in Figure 2 shows that a cathode containing a LiF layer with a thickness exceeding 1.5 nm should provide for a shunt resistance that is sufficiently high (*i.e.* $R_j > 1000\ \Omega$) to allow for the 'faulty' OSC to exhibit near "unflawed" operational characteristics. It is further predicted that for 0.5 nm LiF, despite an increased fill factor, some of the device characteristics should be retained (blue dashed lines in Figure 1) owing to the apparently non-negligible shunt resistance of $R_j = 50\ \Omega$.

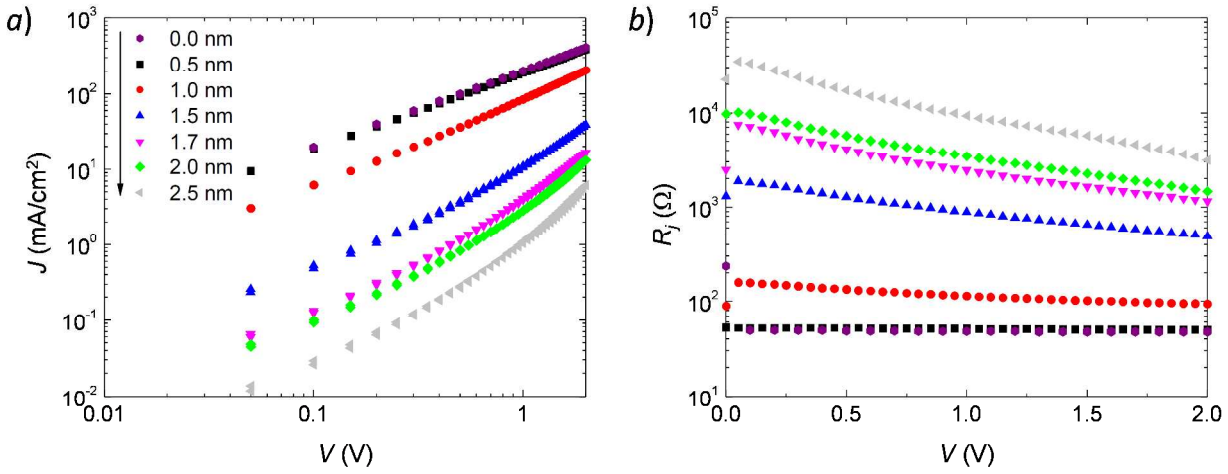

Figure 3. *a) Current density (J) plotted as function of voltage (V) for ITO-PEDOT:PSS-LiF/Al stacks with different nominal LiF thickness (indicated in Figure); the thickness of the aluminum layer is kept constant at 100 nm; b) resistance (R_j) measured across the stacks plotted as a function of voltage.*

Interestingly, upon increasing the LiF thickness a field-induced lowering of the conduction barrier occurs, evidenced by the increasingly more negative slope in the $R_j(V)$ curves (Figure 3b). In order to investigate the charge transport in more detail we extend our electrical characterization of the PEDOT:PSS-LiF/Al junctions by measuring the current density at a given voltage as a function of temperature in the range $160 < T < 296$ K (Figure 4a). For these measurements the nominal LiF thickness is kept constant at 2.5 nm. The plot shows that across the applied voltage range the current density exhibits a significant temperature-dependence, which suggests that charge emission from the PEDOT:PSS-LiF/Al junction is thermally activated. Fitting the data to Arrhenius function (3) (with J_∞ a pre-exponential factor and kT the thermal energy) yields the activation energy E_a as a function of voltage (Figure 4b).

$$J = J_{\infty} \exp\left(-\frac{E_a}{kT}\right) \tag{3}$$

Although a distinct decrease in E_a with voltage is observed, its magnitude (40 – 70 meV) remains well above the activation barrier for charge transport in the PEDOT:PSS itself (*i.e.* E_a = 6.0±0.5 meV).[17] This confirms that we are indeed probing the intrinsic properties of the PEDOT:PSS-LiF/Al interface.

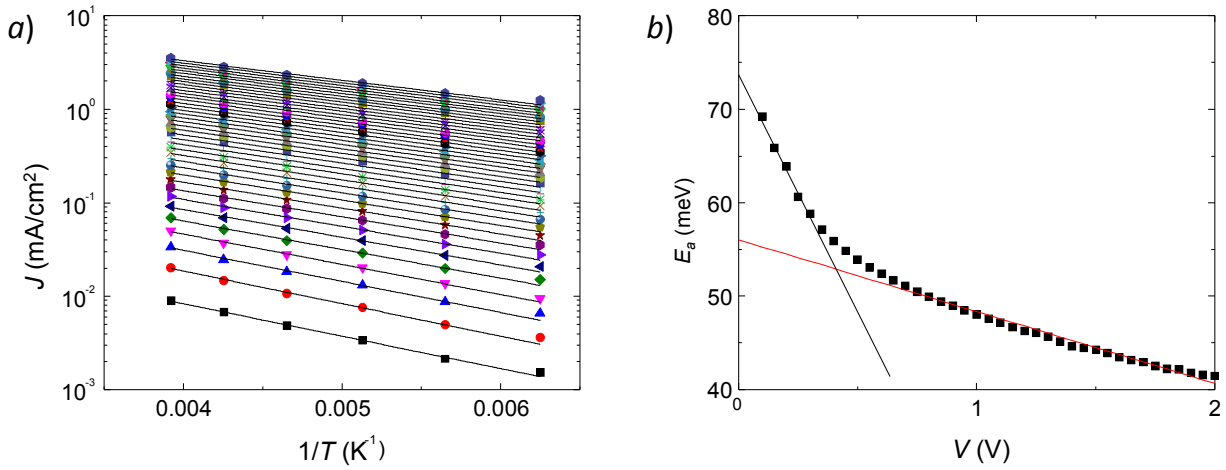

Figure 4. *a) Current density (J) measured at a given voltage across a PEDOT:PSS-LiF/Al junction with d_{LiF} = 2.5 nm plotted as function of reciprocal temperature (1/T); for these measurements the voltage is varied in the range 0.05 – 2 V; the solid lines represent fits to Arrhenius Equation (3); b) activation energy (E_a) obtained from the Arrhenius fits plotted as a function of voltage (V).*

Interestingly, the trend in the observed voltage- (or field-) induced barrier lowering seems to reveal two regimes, as indicated in Figure 4b by the solid lines. The exact mechanism of charge

emission from the PEDOT:PSS-LiF/Al interface is still under investigation and would lead beyond the scope of this work. Nevertheless, the fact that a plot of the current density divided by the voltage (J/V) versus the square root of voltage ($V^{1/2}$) yields a more or less straight line for all temperatures (Figure 5) suggests a Poole-Frenkel-like functionality.[18]

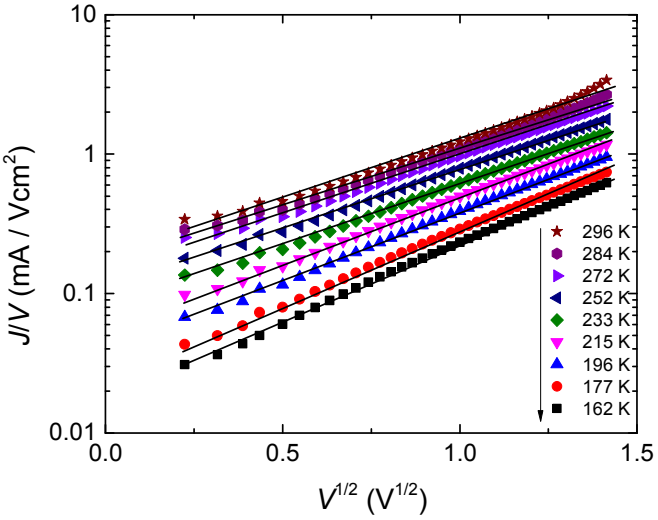

Figure 5. *Current density divided by voltage (J/V) plotted as function of the square root of voltage ($V^{1/2}$), as measured across a PEDOT:PSS-LiF/Al junction (d_{LiF} = 2.5 nm) at different temperatures; the solid lines are guides to the eye indicating Poole-Frenkel-like emission.*

To experimentally verify the above given predictions regarding the operational characteristics of shunted OSCs, we fabricate devices which we intentionally severe by removing a ~10 mm^2 region of the photo-active layer (see experimental section), thus implementing an intentional shunt upon evaporation of the cathode. Figures 6a and 6b show the measured JV-characteristics (symbols) of two such purposely severed devices, again one involving a 2 nm LiF layer and the other a 0.5 nm LiF layer. Comparison of Figure 6 with Figure 1 reveals that only for the 0.5 nm

LiF device the effect of the intentionally created defect is significant. This finding is in excellent agreement with the prediction given above (Figures 2 and 3) which suggest that for a ~10 mm^2 defect a LiF film thickness in excess of 1.5 nm would indeed yield a PEDOT:PSS-cathode junction with a sufficiently high resistance to allow for the OSC to operate more or less normally, in principle making a separate repair procedure prior to cathode deposition redundant. At high negative bias however, shunted OSCs exhibit a higher leakage current than pristine devices, probably as a consequence of the above described Poole-Frenkel-like behavior of the PEDOT:PSS-LiF/Al junction.

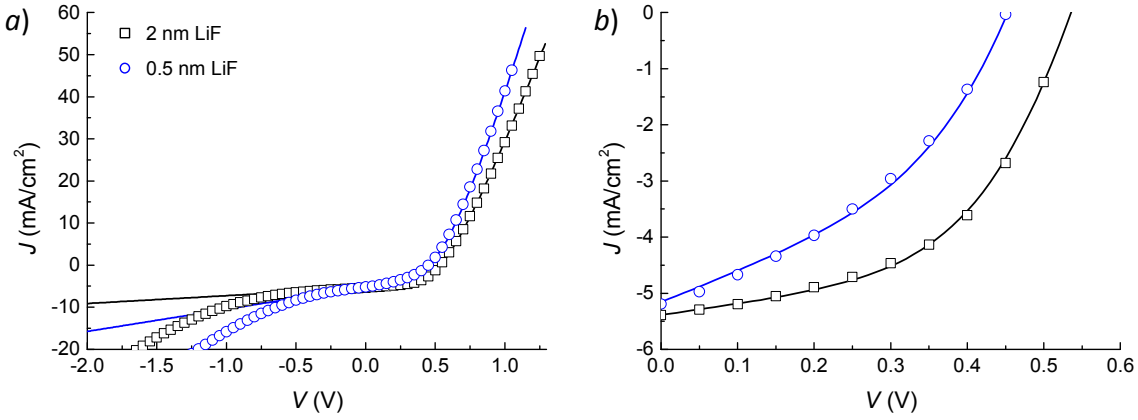

Figure 6. *Current density (J) as function of voltage (V) measured (symbols) for OSCs with a purposely implemented ~10 mm^2 defect in the photoactive having LiF/Al cathodes with 2 nm and 0.5 nm LiF nominal thickness; b) provides a fourth quadrant zoom; the lines represent a best fit to Equation (1).*

Table 2. *Device parameters obtained from curve fitting the JV-data depicted in Figure 6*

d_{LiF} (nm)	V_{oc} (V)	J_{sc} (mA/cm^2)	FF	η (%)	R_s (Ω)	$R_{sh}^{(0)}$ (Ω)	$R_{sh}^{(1)}$ (Ω)	n
2	0.54	-5.39	0.50	1.45	2.8	140	5000	2.8
0.5	0.45	-5.16	0.39	0.89	2.1	140	70	3.0

As is done for the non-severed devices we include lines in Figure 6 representing a best fit of the *JV*-data to Equation (1), this time involving the additional parameter $R_{sh}^{(1)}$ to represent the effect of the intentionally implemented defect. In order to determine whether the observed values for the resistance (R_j) of the PEDOT:PSS-LiF/Al junction indeed provide a measure for the resistance of the short circuit in an OSC, we predefine $R_{sh}^{(1)}$ based on the data in Figure 3b at effective (mean) values of 5000 Ω and 70 Ω, corresponding to the 2 nm and 0.5 nm LiF cathode. Other parameters are optimized in the fitting procedure (see Table 2) and are found to be in the same range as the values obtained for the non-severed devices, with, as expected, the open circuit voltage, fill factor and efficiency of the severed 0.5 nm LiF device as notable exceptions.

We finally note that devices with a 0.5 nm nominal LiF thickness are occasionally affected less negatively by the shunt than expressed by Figure 6, most likely due to sample-to-sample variation in the effective thickness of the LiF layer. In case of 2 nm LiF devices, samples manufactured in different batches consistently exhibit unaltered fourth quadrant characteristics as compared to pristine OSCs. These observations are in agreement with results by Brabec *et al.* showing a decrease of the sample-to-sample variation in device performance with increasing LiF film thickness.[16]

4. Conclusions

Using a simple equivalent circuit model involving a diode, a series resistance and a parallel shunt resistance we predict that short-circuits in conventional organic solar cells due to defects in the photoactive layer have little to no effect on device performance as long as their resistance is higher than 1000 Ohms. By measuring the resistance of PEDOT:PSS-LiF/Al cathode junctions, as encountered in such defects, we show that even for shunts with macroscopic lateral dimensions (~10 mm^2) this prerequisite is met when a LiF layer is applied with a thickness exceeding 1.5 nm. At lower thickness values the shunt resistance significantly decreases, leading to a considerable drop in the predicted fill factor. For LiF layers in excess of 1.5 nm the current density increases super-linearly with voltage due to a Poole-Frenkel-like behavior of the charge emission from the PEDOT:PSS-LiF/Al interface. The predictions have been experimentally validated by comparing the calculated *JV*-curves with measured ones involving OSCs with purposely severed photoactive layers and various LiF layer thicknesses. The excellent agreement between theory and experiment, together with our analysis on charge emission through shunted regions, shows that i) the effect of a shunt in the photoactive region of a conventional OSC is sufficiently well understood to in principle allow for the prediction of fault-tolerance levels of the light-to-power conversion efficiency, and ii) the resilience of OSCs against processing imperfections or damage to the photoactive layer is considerably enhanced by applying a cathode containing a relatively thick LiF layer.

Acknowledgements

The research leading to these results has received funding from the Netherlands Enterprise Agency and the European Union's Seventh Framework Program (FP7/2007-2013) under grant

agreement n° 281027. The authors would like to thank Ton van den Biggelaar (Philips Eindhoven) for the precise evaporation of thin LiF layers. We further acknowledge Dr. T. van Gijseghem (AGFA Gevaert) for supplying highly conductive PEDOT:PSS.

REFERENCES

[1] R. Søndergaard, M. Hösel, and F.C. Krebs, *J. Polym. Sci., Part B: Polym. Phys,* 2013, **51**, 16.

[2] K. Müllen, and U. Scherf, in Organic Light-Emitting Devices, John Wiley & Sons, New York, 2006.

[3] R. Søndergaard, M. Hösel, D. Angmo, T.T. Larsen-Olsen and F.C. Krebs, *Mater. Today,* 2012, **15**, 36.

[4] M. Nagai, *J. Electrochem. Soc.* 2007, **154**, J387.

[5] L. Xue, Y. Han, *Progr. Mater. Sci.*, 2012, **57**, 947.

[6] A. J. Oostra, P.W.M. Blom and J. J. Michels, *Org. Electron.* 2014, **15**, 1166.

[7] A. J. Oostra, P.W.M. Blom and J. J. Michels, *Sol. Energ. Mat. Sol. Cells,* 2015, **134**, 334.

[8] A. J. Oostra, K. H. W. van den Bos, P. W. M. Blom, and J. J. Michels, *J. Phys. Chem. B.,* 2013*,* **117**, 10929.

[9] S. S. Hegedus and W. N. Shafarman, *Prog. Photovoltaics*, 2004, **12**, 155.

[10] S. M. Sze and K. K. Ng, *Physics of Semiconductor Devices*, 3rd ed. (Wiley, New York, 2006).

[11] J. Shi, J. Dong, S. Lv, Y. Xu, L. Zhu, J. Xiao, X. Xu, H. Wu, D. Li, Y. Luo and Q. Meng, *Appl. Phys. Lett.*, 2014, **104**, 063901.

[12] To avoid confusion: here we refer to the current density of the cell at zero bias and not to the current through a short circuit in the active stack.

[13] M. Jørgensen, J. E. Carlé, R. R. Søndergaard, M. Lauritzen, N. A. Dagnaes-Hansen, S. L. Byskov, T. R. Andersen, T. T. Larsen-Olsen, A. P. L. Böttiger, B. Andreasen, L. Fu, L. Zuo, Y. Liu, E. Bundgaard, X. Zhan, H. Chen and F. C. Krebs, *Sol. Energ. Mat. Sol. Cells,* 2013, **119**, 84.

[14] M. Wang, Y. Li, H. Huang, E. D. Peterson, W. Nie, W. Zhou, W. Zeng, W. Huang, G. Fang, N. Sun, X. Zhao and D. L. Carroll, *Appl. Phys. Lett.* 2011, **98**, 103305.

[15] H. Heil, J. Steiger, S. Karg, M. Gastel, H. Ortner, H. von Seggem and M. Stößel, *J. Appl. Phys.,* 2001, **89**, 420.

[16] C. J. Brabec, S. E. Shaheen, C. Winder, N. S. Sariciftci, and P. Denk, *Appl. Phys. Lett.*, 2002, **80**, 1288.

[17] A. M. Nardes, M. Kemerink, and R.A.J. Janssen, *Phys. Rev. B.* 2007, **76**, 085208.

[18] S.M. Sze, in Physics of Semiconductor Devices, John Wiley & Sons, New York, 2nd edn, 1981.